ENVIRONMENTAL EMBRITTLEMENT OF POLYSYNTHETICALLY TWINNED (PST) CRYSTALS OF BINARY AND SOME TERNARY TiAl COMPOUNDS

H. INUI AND M. YAMAGUCHI
Department of Metal Science and Technology, Kyoto University, Sakyo-ku, Kyoto 606, Japan.

ABSTRACT

Environmental effects on the room temperature ductility of polysynthetically twinned (PST) crystals of binary and some ternary TiAl compounds have been investigated through tensile tests conducted in four different atmospheres. The tensile ductility of TiAl PST crystals is sensitive to test environment. It is higher when tested in vacuum or in dry air than in air or in hydrogen gas. The environmental embrittlement of binary TiAl PST crystals can be thus interpreted in terms of hydrogen embrittlement. The environmental loss in ductility of PST crystals decreases with increasing strain rate. The fracture mode also depends on test environment and strain rate. When the environmental loss is larger, that is when tested in air or in hydrogen gas at lower strain rates, they fail in a cleavage-like mode with a habit plane parallel to the lamellar boundaries. Otherwise, fracture occurs across the lamellar boundaries.The ternary TiAl PST crystals containing Cr, Mn or Mo exhibit higher ductility than the binary TiAl PST crystals when tested in air, while the ternary ones show lower ductility than the binary ones in vacuum. In the ternary TiAl PST crystals, fracture occurs across the lamellar boundaries both in air and in vacuum. Additions of alloying elements such as Cr, Mn and Mo seem to be effective in reducing the environmental loss in ductility of TiAl PST crystals. Based on the results obtained, possible mechanisms of environmental embrittlement in two-phase TiAl compounds are discussed.

INTRODUCTION

Ti-rich TiAl compounds with the two-phase TiAl/Ti_3Al lamellar structure have been of considerable interest in the last few years as a new class of high-temperature structural materials [1-3]. One of the major limitations for the practical use of the compounds is the poor ductility at ambient temperature. Thus, many of recent studies on two-phase TiAl compounds have been focused on the improvement of their limited ductility [1,2,4]. On the other hand, recent researches on intermetallic compounds such as Ni_3Al and FeAl have shown that environmental embrittlement can be a possible reason for a limited ductility at ambient temperature [5]. Although there is some evidence to indicate that TiAl-based compounds are susceptible to environmental embrittlement [6,7], it is difficult to reliably measure the difference in tensile elongation of two-phase TiAl compounds between in air and in vacuum since they exhibit only

a limited ductility in polycrystalline form [8-10]. With the use of so-called polysynthetically twinned (PST) crystals of TiAl in which only a single grain with the TiAl/ Ti_3Al lamellar structure is contained, we have made a systematic study on the deformation behavior as a function of the angle (ϕ) between the lamellar boundaries and loading axis [11-15] and demonstrated that a tensile elongation as large as 20% can be obtained in air at room temperature for ϕ=31° where the easy type of deformation (shear deformation parallel to the lamellar boundaries) occurs [13]. This is far larger than any other values of room temperature ductility ever reported on two-phase TiAl compounds. We have thus decided to investigate environmental effects on the ductility of two-phase TiAl compounds using PST crystals to see whether the environmental embrittlement plays a role in limiting their ductility.

In this paper, we report the deformation behavior of binary and some ternary TiAl PST crystals in tension at room temperature in four different atmospheres and demonstrate that the two-phase TiAl compounds are susceptible to environmental embrittlement.

A BRIEF SUMMARY OF OUR PREVIOUS STUDY ON THE TENSILE DEFORMATION OF PST CRYSTALS OF TiAl IN AIR

In our previous paper [11,13], we have reported the results of a systematic study on the room-temperature deformation behavior of PST crystals with nine different orientations in air at a stain rate of $2.0 \times 10^{-4} s^{-1}$. A brief summary of the previous results [13], in particular, those on the room-temperature ductility and fracture behavior of TiAl PST crystals in air will be given in the following.

(1) The tensile elongation to fracture as well as the yield stress strongly depend on the angle ϕ.

(2) A tensile elongation as large as 20% can be achieved in specimens with orientation B_1 (ϕ=31°) in which the easy type of deformation occurs.

(3) The largest values of tensile elongation observed for specimens with orientation A_1 (ϕ=0°) and N (ϕ=90°) where the hard type of deformation (shear deformation across the lamellar boundaries) occurs are 12% and 1%, respectively.

(4) There is no significant difference in deformation modes between tension and compression, i.e. the major deformation modes of PST crystals of TiAl are true twinning of the {111}<112]-type and slip along <110] both in tension and compression.

(5) Fracture always occurs in a brittle manner without showing any local contraction even in specimens exhibiting a tensile elongation as large as 20%. However, two distinct types of fracture behavior can be observed depending on the angle ϕ. When the tensile axis is parallel to the lamellar boundaries, a crack propagates in a zigzag across the lamellar boundaries while in cases where the tensile axis is perpendicular or inclined to the lamellar boundaries, fracture occurs in a cleavage-like mode with a habit plane parallel to the lamellar boundaries.

On the basis of these results, we selected specimens with orientation B_1 (ϕ=31°) for the present study to investigate the environmental effects on the tensile deformation behavior.

EXPERIMENTAL

Compositions of the master ingots used in the present study were Ti-49.3at.%Al and Ti-48.4at.%Al-0.6at.%X (X=Cr, Mo and Mn), respectively. Binary and ternary TiAl PST crystals, 10 mm in diameter and 100 mm long, were grown from the master ingots using an ASGAL FZ-SS35W optical floating zone furnace. Oriented tensile specimens with ϕ=31° (orientation B_1), approximately 2 mm x 0.5 mm in cross section and 5 mm in gauge length, were cut from as grown PST crystals. These specimens were polished first mechanically and then electrolytically to remove surface damage prior to tensile tests. Tensile tests were conducted at room temperature in the strain rate range of $2.0\text{x}10^{-4}\text{s}^{-1}$ to $1.0\text{x}10^{-1}\text{s}^{-1}$, using an Instron-type testing machine equipped with a vacuum chamber. Four different atmospheres were employed; air, vacuum, dry air (an artificial mixture of 79% nitrogen and 21% oxygen gas) and dry hydrogen gas. Tensile tests in vacuum were conducted in the chamber dynamically pumped to a vacuum better than $1\text{x}10^{-3}$ Pa. For tensile tests in a gas atmosphere, the chamber was first evacuated to $1\text{x}10^{-3}$ Pa and then the desired gas was introduced to the chamber until the gas pressure reached 1 atm (≈0.1 MPa). Deformation structures were examined by optical microscopy and transmission electron microscopy (TEM). Fracture surfaces were examined by scanning electron microscopy (SEM).

RESULTS

Binary TiAl PST crystals

Figure 1 shows stress-strain curves obtained at three different strain rates in four different atmospheres. The stress-strain curves shown in Fig. 1 are those for specimens with the largest elongation for each testing condition. As seen in Fig. 1, the yield stress and work-hardening rate are almost insensitive to test environment and strain rate but the tensile ductility and the fracture stress are sensitive to both test environment and strain rate. For example, at the lowest strain rate of $2.0\text{x}10^{-4}\text{s}^{-1}$, the value of tensile elongation observed in vacuum is as large as 56% which is far larger than those in air (20%) and in hydrogen gas (11%). However, at the highest strain rate of $1.0\text{x}10^{-1}\text{ s}^{-1}$, the tensile elongation in vacuum decreases to 35%, which is comparable to those in air (36%) and in hydrogen gas (30%). Figure 2 collectively shows the strain rate dependence of the tensile elongation, fracture stress and yield stress in each atmosphere. When tested in vacuum, the tensile elongation and fracture stress decrease with increasing strain rate. In contrast, the tensile elongation and fracture stress increase with increasing strain rate in air and in hydrogen gas. Thus, the environmental loss in ductility of

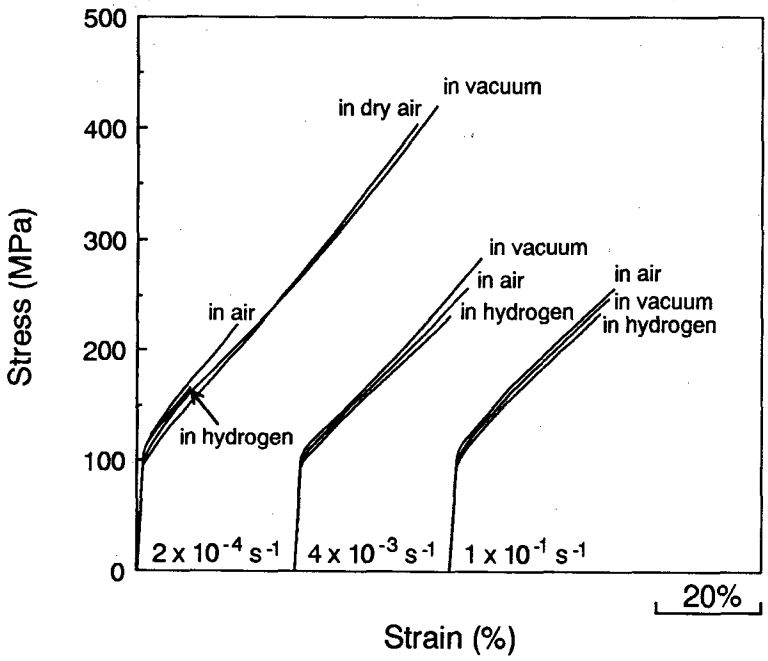

Figure 1. Stress-strain curves obtained for binary TiAl PST crystals at three different strain rates in four different atmospheres [14].

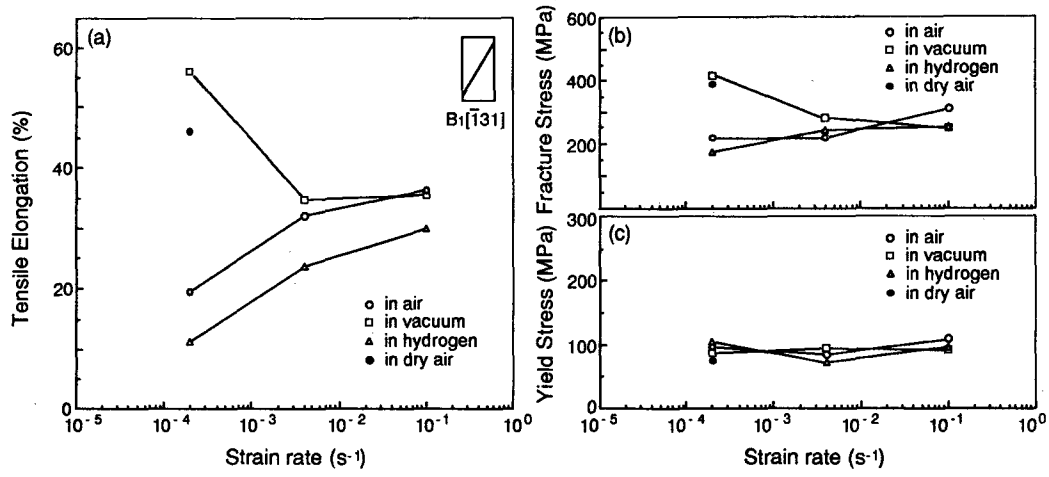

Figure 2. Strain rate dependence of tensile elongation (a), fracture stress (b) and yield stress (c) of binary TiAl PST crystals [14].

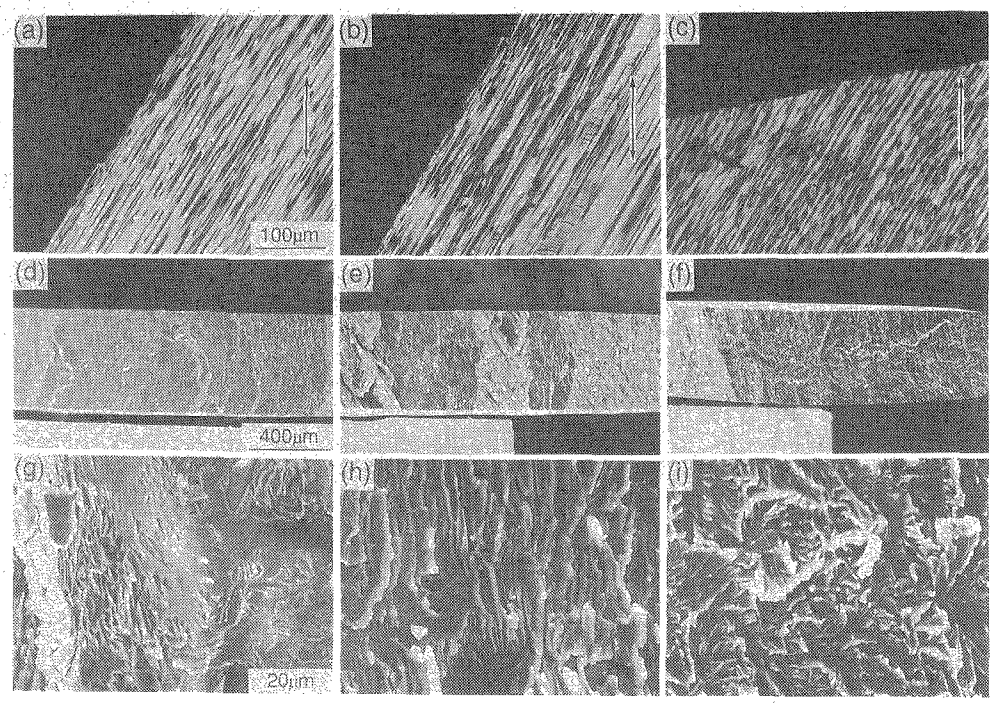

Figure 3. Side (a-c) and top (d-i) views of fracture surfaces of binary TiAl PST crystals tested in air (a,d,g), in hydrogen gas (b,e,h) and in vacuum (c,f,i), respectively, at the lowest strain rate of $2.0 \times 10^{-4} s^{-1}$. The tensile axis is shown by arrows in the figures [14].

PST crystals of TiAl decreases with increasing strain rate, indicating that a diffusion process contributes to the embrittlement. The environmental loss in ductility is larger when tested in hydrogen gas than in air for all the strain rates used. In dry air at the lowest strain rate of $2.0 \times 10^{-4} s^{-1}$, the tensile elongation is 46%, which is somewhat smaller than that in vacuum but much larger than those observed in air and in hydrogen gas. This indicates that the environmental embrittlement in air may be due to moisture-induced hydrogen. Thus, the environmental embrittlement in TiAl may be interpreted in terms of hydrogen embrittlement.

When tested at the lowest strain rate at which the environmental loss in ductility is largest, two distinct types of fracture modes were observed depending on test environment. Figures 3(a)-(c) show side views of fracture surfaces of specimens tested in air, in hydrogen gas and in vacuum, respectively. The values of tensile elongation of specimens shown in Figs. 3(a)-(c) were 20%, 11% and 56%, respectively. In air and in hydrogen gas, fracture occurs in a cleavage-like mode with a macroscopic habit plane parallel to the lamellar boundaries, whereas fracture occurs across the lamellar boundaries when tested in vacuum. The fracture mode observed in specimens tested in dry air was essentially similar to that observed in specimens

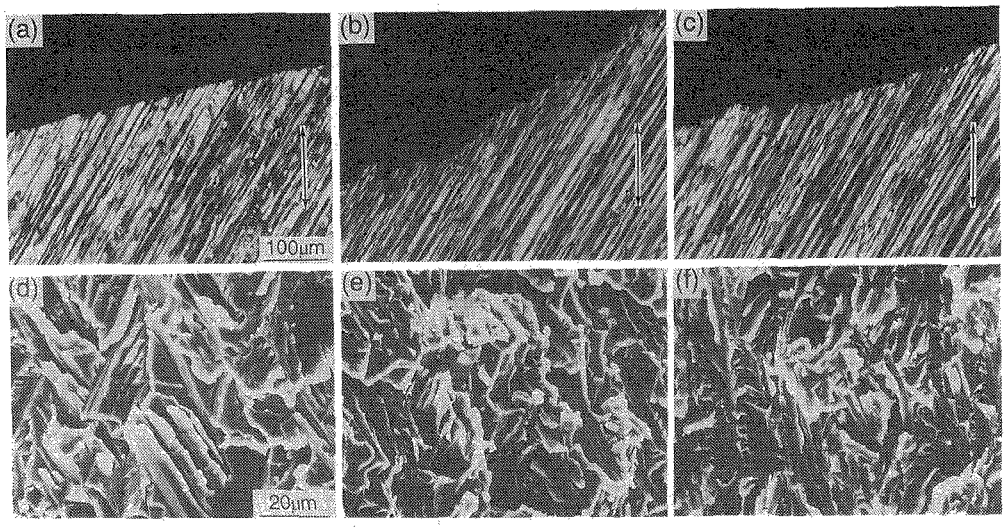

Figure 4. Side (a-c) and top (d-f) views of fracture surfaces of binary TiAl PST crystals tested in air (a,d), in hydrogen gas (b,e) and in vacuum (c,f), respectively, at the highest strain rate of $1.0x10^{-1}s^{-1}$. The tensile axis is shown by arrows in the figures [14].

tested in vacuum. Of interest to note in Fig. 3(c) is that fracture occurs in a brittle manner without showing any local contraction even after deformed to 56% in vacuum.

Top views of fracture surfaces of specimens of Figs. 3(a)-(c) are presented in Figs. 3(d) -(f) at a low magnification and (g)-(i) at a high magnification, respectively. Specimens tested in air (a) and in hydrogen gas (b) exhibit a flat fracture surface composed of terraces of various sizes with the terrace plane parallel to $(111)_{TiAl}$, whereas those tested in vacuum (c) show a relatively rough and tortuous fracture surface. The environmental loss in ductility decreases with increasing strain rate as shown in Figs. 1 and 2, and the fracture behavior becomes accordingly less dependent on test environment with increasing strain rate. Therefore, at higher strain rates, cracks propagate not parallel to the lamellar boundaries but across the lamellar boundaries regardless of test environment. Figures 4(a)-(c) respectively show side views of fracture surfaces of specimens tested in air, in hydrogen gas and in vacuum at the highest strain rate of $1.0x10^{-1}s^{-1}$. The values of tensile elongation of specimens shown in Figs. 4(a)-(c) were 36%, 30% and 35%, respectively. At this strain rate, cracks propagate not parallel to the lamellar boundaries but across them regardless of test environment. SEM observations of top views of fracture surfaces clearly reveal the occurrence of rough and tortuous translamellar fracture in all the cases (Figs. 4(d)-(f)).

The environmental loss in ductility of binary TiAl PST crystals which deform by the easy type of deformation is clearly related to the change in fracture mode. When the

environmental loss in ductility is large, PST crystals of TiAl fail by a cleavage-like mode with a habit plane parallel to the lamellar boundaries. Otherwise, fracture occurs across the lamellar boundaries.

Ternary TiAl PST crystals

Figures 5(a)-(c) show stress-strain curves obtained in air and in vacuum for binary and ternary TiAl PST crystals containing Cr and Mo, respectively. The tensile tests were conducted at the lowest strain rate of $2.0x10^{-4}s^{-1}$ at which the largest environmental loss in ductility was observed for binary TiAl PST crystals. The stress-strain curves shown in Fig. 5 are those for specimens with the largest elongation for each testing condition. As in the case of binary PST crystals, the tensile elongation of ternary PST crystals is sensitive to test environment; it is higher when tested in vacuum than in air. When tested in air, the values of tensile elongation obtained for ternary PST crystals doped with Cr and Mo are respectively 35% and 28%, which

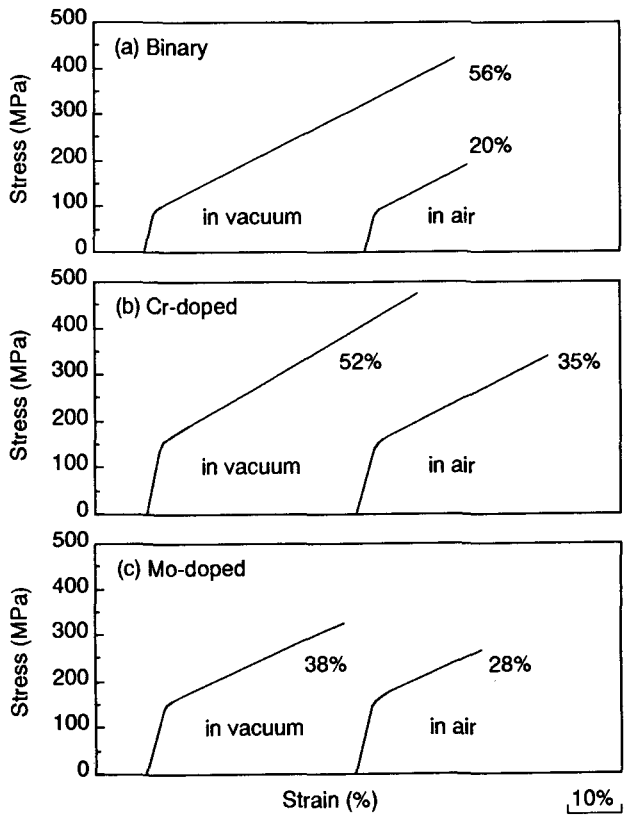

Figure 5. Stress-strain curves obtained for binary and ternary TiAl PST crystals tested in air and in vacuum at the lowest strain rate of $2.0x10^{-4}s^{-1}$ [15].

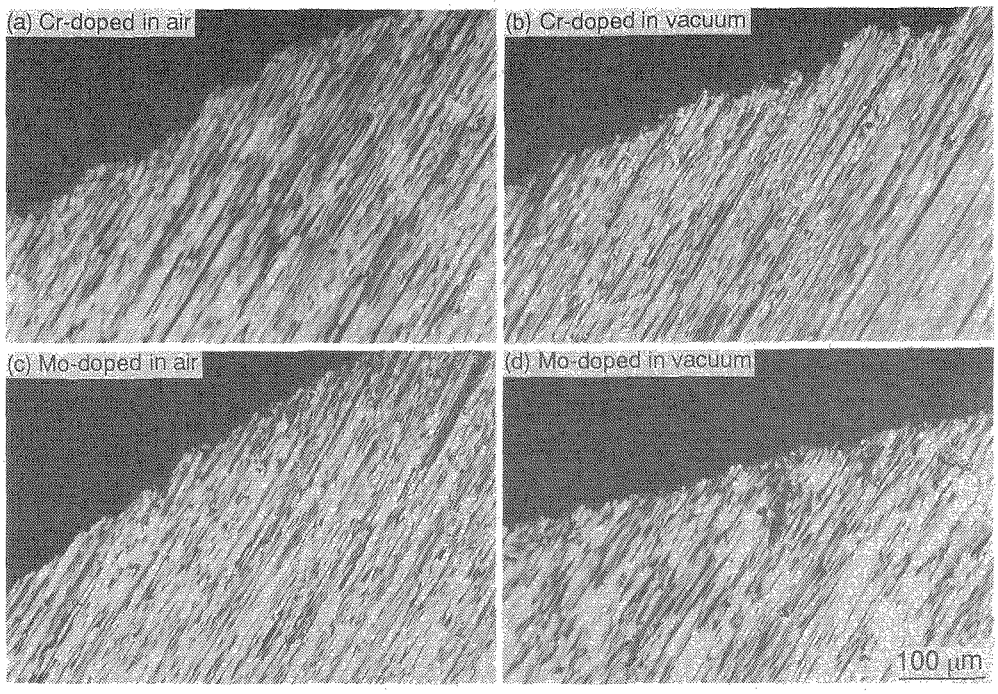

Figure 6. Side views of fracture surfaces of Cr- (a,b) and Mo-doped (c,d) ternary TiAl PST crystals tested in air (a,c) and in vacuum (b,d) at the lowest strain rate of $2.0 \times 10^{-4} s^{-1}$ [15].

are larger than that for binary PST crystals (20%). This result is coincident with the recent reports on the beneficial effects of ternary alloying additions on the room temperature ductility of polycrystalline two-phase TiAl compounds [1,2,4]. In contrast, when tested in vacuum, the values of tensile elongation obtained for ternary PST crystals (52% and 38% for Cr- and Mo-doped, respectively) are lower than that for binary PST crystals (56%). The same trend in tensile ductility was observed also for Mn-doped ternary PST crystals.

Figures 6(a)-(d) show side views of fracture surfaces of Cr- (a,b) and Mo-doped (c,d) ternary specimens tested at the lowest strain rate of $2.0 \times 10^{-4} s^{-1}$ in air (a,c) and in vacuum (b,d), respectively. As seen in the figures, fracture occurs across the lamellar boundaries regardless of test environment for ternary PST crystals doped with Cr and Mo. In contrast, fracture occurs in a cleavage-like mode with a habit plane parallel to the lamellar boundaries for binary PST crystals tested in air (Fig 3(a)). Thus, the increased tensile ductility of ternary PST crystals in air is related to the change in fracture mode.

All these facts indicate that the increase in tensile ductility of the ternary PST crystals in air is due to the reduction in the environmental loss in ductility but not due to the enhancement of deformation modes. In fact, TEM examinations of deformation structures made on binary and ternary PST crystals tested in air and in vacuum have revealed no significant difference,

i.e., the major deformation modes are deformation twinning of the {111}<112]-type and slip along <110] for all the cases.

DISCUSSION

The tensile ductility of binary TiAl PST crystals is higher when tested in vacuum or in dry air than in air or in hydrogen gas. The environmental loss in ductility decreases with increasing strain rate. Such features are essentially similar to those observed in many intermetallic compounds which are susceptible to environmental embrittlement [5]. Thus, the environmental embrittlement of two-phase TiAl compounds may be interpreted in terms of hydrogen embrittlement as in many intermetallic compounds. It is known that Ti_3Al-based alloys are susceptible to hydrogen embrittlement [16-21]. When Ti_3Al-based alloys like super α_2 are cathodically or thermally charged with hydrogen prior to tests, embrittlement occurs due to the formation of hydrides [19,20]. Severe embrittlement of super α_2 has been reported to occur also in 34.5 MPa hydrogen gas at 25℃ and 204℃ [21]. Hydride formation has been also reported in some TiAl-based compounds cathodically or thermally charged with hydrogen [22]. However, in the present case hydride formation was not observed in any of deformed PST crystals by TEM observations [13,14]. This clearly indicates that the environmental embrittlement of TiAl PST crystals may not be attributed to hydride formation, in contrast to the case of Ti_3Al-based alloys. No significant difference in deformation structure was observed between specimens deformed in air or in hydrogen gas and those in vacuum at any strain rates. That is, the major deformation modes are true twinning of the {111}<112]-type and slip along <110] regardless of test environment, as we previously reported [12,13]. Thus, the observed environmental loss in ductility can not be ascribed to the the change in deformation mode. Many investigations of hydrogen embrittlement in intermetallics have postulated that a decohesion mechanism, in which the lowering of bonding strength occurs in the presence of hydrogen gas, is responsible for the embrittlement [5]. As shown in Fig. 3, binary PST crystals fail by a cleavage-like mode with a habit plane parallel to the lamellar boundaries when the environmental loss in ductility is large, that is when tested in air and in hydrogen gas at lower strain rates, otherwise fracture occurs across the lamellar boundaries. This indicates that the embrittlement of binary PST crystals can be also explained by a decohesion model in which the bonding strength along the lamellar boundaries is lowered in the presence of hydrogen gas.

We now discuss the mechanisms of the environmental embrittlement which occurs preferentially along the lamellar boundaries in TiAl PST crystals. Due to the presence of six different types of ordered domains in the TiAl phase, three different types of lamellar domain boundaries can exist in the TiAl lamellae [23,24]; (I) true-twin type (energy:γ_T), (II) pseudo-twin type (energy:γ_P) and (III) 120°-rotational order-fault type (energy:γ_R). These are schematically illustrated in Figs. 7(a)-(c). In the figures, closed, open and hatched circles

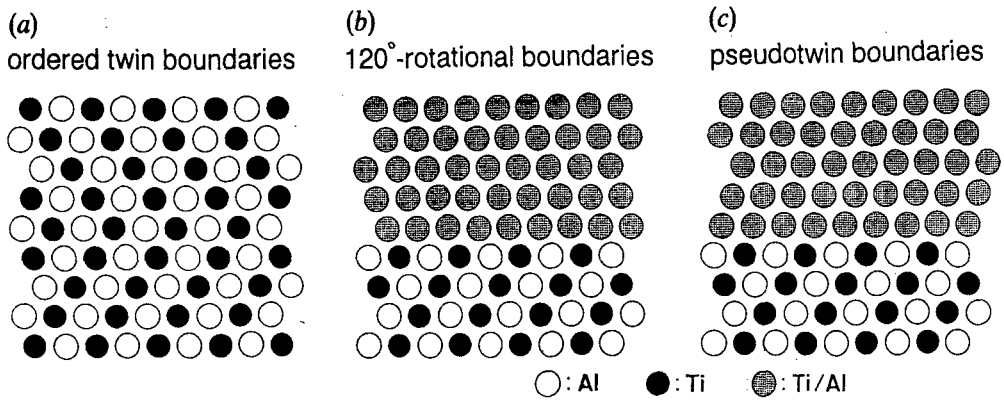

Figure 7. Schematic illustrations of ordered twin boundaries (a), 120°-rotational boundaries (b) and pseudotwin boundaries (c).

respectively represent atomic rows composed of Ti atoms only, Al atoms only and alternatively arranged Ti and Al atoms. The energies of these boundaries, considering the first-, and second-nearest neighbor interactions only on the basis of a hard-sphere model, in an AB compound with the L1$_0$ structure are respectively

$$\gamma_T = \frac{2[\phi_{AA}(r') + \phi_{BB}(r')]}{3^{1/2}a^2}, \tag{1}$$

$$\gamma_R = \frac{(2V^{(1)} - 6V^{(2)})}{3^{1/2}a^2}, \tag{2}$$

$$\gamma_P = \gamma_R + \frac{[\phi_{AA}(r') + \phi_{BB}(r') + 2\phi_{AB}(r')]}{3^{1/2}a^2}$$

$$\approx \gamma_R + \gamma_T. \tag{3}$$

where the slight tetragonality of the L1$_0$ structure is neglected and $\phi_{ij}(r')$ is the interaction energy between i and j atoms at the separation $r'=(2/3^{1/2})a$ where a is the lattice parameter. $V^{(k)}=(\phi_{AA}+\phi_{BB}-2\phi_{AB})/2$ and ϕ_{ij} are the pairwise interaction energies between k th-neighbor atoms. Using the values of $\gamma_{APB}/\gamma_{SISF}$ obtained theoretically (~6) [25,26] and experimentally (~2) [27], the ratio of energies of these three boundaries (γ_T, γ_P and γ_R) has been estimated to be in the range of 1:3:2 or 1:7:6 [24], where γ_{APB} and γ_{SISF} are the energy of the antiphase boundary (APB) on {111} with a fault vector of 1/2<101] and that of the superlattice intrinsic stacking fault on {111}, respectively. In accord with the estimate, true-twin boundaries are most frequently observed. However, the other two types of boundaries are also often observed. This suggests that the lamellar domain boundaries of pseudo-twin and 120°-rotational types may

have much smaller energies than those estimated on the basis of a hard-sphere model [16] most probably due to the relaxation of atoms in the close vicinity to the fault plane. Otherwise, the lattice mismatches would generate huge elastic stresses at the lamellar domain boundaries of these two types [28] and they may not exist in the TiAl phase. Thus, the lamellar domain boundaries of the pseudo-twin and the 120°-rotational types would involve such relaxations of atoms and may have potential to accept hydrogen atoms along them, offering the preferential path for hydrogen penetration. Then, the bond strength of these boundaries will be reduced in the presence of hydrogen, resulting in a cleavage-like fracture along them, that is, parallel to the lamellar boundaries. The environmental embrittlement in TiAl PST crystals can thus be understood in terms of the high susceptibility of the pseudo-twin and 120°-rotational lamellar domain boundaries to hydrogen attack.

These lamellar domain boundaries should have potential to accept not only hydrogen atoms but also ternary alloying atoms. In fact, as shown in Fig.6, PST crystals of TiAl vary in the room-temperature fracture mode from cleavage-like parallel to the lamellar boundaries to cracking in zigzag across the lamellar boundaries by adding ternary alloying elements such as Cr, Mn and Mo, and their environmental embrittlement is reduced as a result. This may be because ternary alloying atoms segregate preferentially to the pseudo-twin and 120°-rotational lamellar domain boundaries and reduce their vulnerability to hydrogen attack. Indeed, segregation of Mn atoms to lamellar boundaries has been observed by field ion microscopy (FIM) [29].

CONCLUSIONS

(1) TiAl PST crystals are susceptible to environmental embrittlement. The tensile ductility of TiAl PST crystals is higher when tested in vacuum or in dry air than in air or in hydrogen gas. Thus, the embrittlement can be interpreted in terms of hydrogen embrittlement.

(2) The environmental loss in ductility decreases with increasing strain rate. When the environmental loss is large, that is when tested in air or in hydrogen gas at lower strain rate, binary TiAl PST crystals fail in a cleavage-like mode with a habit plane parallel to the lamellar boundaries, otherwise fracture occurs across the lamellar boundaries.

(3) Ternary TiAl PST crystals containing Cr, Mn and Mo exhibit higher ductility than the binary TiAl PST crystals when tested in air, while the ternary ones show lower ductility than the binary ones in vacuum. The ternary TiAl PST crystals fail by cracking across the lamellar boundaries regardless of test environment. Thus, the increase in tensile ductility of the ternary PST crystals can be interpreted in terms of the reduction in the environmental loss in ductility of TiAl PST crystals.

ACKNOWLEDGEMENTS

This work was supported by Grant-in-Aid for Scientific Research on the priority Area "Intermetallic compounds as New High Temperature Structural Materials" from the Ministry of Education, Science and Culture, Japan and in part by the research grant from R & D Institute of Metals and Composites for Future Industries. The authors would like to thank M. H. Oh, M. Kobayashi and M. Misaki for their help in experiments.

REFERENCES

[1] Y.W. Kim and D.W. Dimiduk, JOM, 1991, 43 (8), 40 .
[2] S.C. Huang and D.S. Shih, In Microstructure/Property Relationships in Titanium Aluminides and Alloys, ed. Y.W. Kim and R.R. Boyer, TMS, Warrendale, 1991, p. 105.
[3] M. Yamaguchi and H. Inui, In Ordered Intermetallics-Physical Metallurgy and Mechanical Behavior, ed. C.T. Liu, R.W. Cahn and J.O. Sauthoff, Kluwer Academic Publishers, Dordrecht, 1992, p. 217.
[4] T.Tsujimoto and K. Hashimoto, In High-Temperature Ordered Intermetallic Alloys III, ed. C.T. Liu, A.I.Taub, N.S. Stoloff and C.C. Koch, Mater. Res. Soc., Pittsburgh, 1989, p. 391.
[5] for example, C.T. Liu and C.G. McKamey In High Temperature Aluminides and Intermetallics, ed. S.H. Whang, C.T. Liu, D.P. Pope and J.O. Stiegler, TMS, Warrendale, 1990, p. 133.
[6] C.T. Liu and Y.W. Kim, Scripta Metall. Mater., 1992, 27, 599.
[7] T. Takasugi, S. Hanada and M. Yoshida, J. Mater. Res., 1992, 7, 2739.
[8] R.D. Kane and E.A. Chakachery, In Environmental Effects on Advanced Materials, ed. R.H. Jones and R.E. Ricker, TMS, Warrendale, 1991, p. 35.
[9] D.A. Meyn, In Microstructure/Property relationships in Titanium Aluminides and Alloys, ed. Y.W. Kim and R.R. Boyer, TMS, Warrendale, 1991, p. 275.
[10] W. Y. Chu and A. W. Thomson, Scripta Metall. Mater., 1991, 25, 2133.
[11] T. Fujiwara, A. Nakamura, M. Hosomi, S.R. Nishitani, Y. Shirai and M. Yamaguchi, Phil. Mag. A, 1990, 61, 591.
[12] H. Inui, A. Nakamura, M.H. Oh and M. Yamaguchi, Phil. Mag. A, 1992, 66, 557.
[13] H. Inui, M.H. Oh, A. Nakamura and M. Yamaguchi, Acta Metall. Mater., 1992, 40, 3095.
[14] M.H. Oh, H. Inui, M. Misaki and M. Yamaguchi, Acta Metall. Mater., 1993, in press.
[15] M.H. Oh, H. Inui, M. Misaki, M. Kobayashi and M. Yamaguchi, In High-Temperature Ordered Intermetallic Alloys V, ed. I. Baker, J.D. Whittenberger, R. Darolia and M.H. Yoo, Mater. Res. Soc., Pittsburgh, 1993, in press.
[16] D.S. Shih, G.K. Scarr and G.E. Wasielewski, In Proc. 2nd Workshop on Hydrogen-Materials Interactions, ed. H.G. Nelson, NASA Workshop Publication, 1988, p.1004.
[17] D.S. Shih, G.K. Scarr and G.E. Wasielewski, Scripta Metall. Mater., 1989, 23, 973.
[18] M. Gao, J.B. Boodey and R.P. Wei, In Proc. 3rd Workshop on Hydrogen-Materials Interactions, ed. H.G. Nelson, NASA Workshop Publication, 1990, p. 1007.
[19] W.Y. Chu, A.W. Thomson and J.C. Williams, In Hydrogen Effects on Material Behavior, ed. N.R. Moody and A.W. Thomson, TMS, Warrendale, 1990, p. 543.
[20] E. Monor and D. Eliezer, Scripta Metall. Mater., 1990, 24, 129.
[21] S. Sullivan, In Proc. 2nd Workshop on Hydrogen-Materials Interactions, ed. H.G. Nelson, NASA Workshop Publication, 1988, p.1004.
[22] D. Legzdina, I.M. Robertson and H.K. Birnbaum, J. Mater. Res., 1991, 6, 1230.
[23] H. Inui, A. Nakamura, M.H. Oh and M. Yamaguchi, Ultramicroscopy, 1991, 39, 298.
[24] H. Inui, M.H. Oh, A. Nakamura and M. Yamaguchi, Phil. Mag. A, 1992, 66, 539.
[25] C.L. Fu and M.H. Yoo, Phil. Mag. Lett., 1990, 62, 159.

[26] C. Woodward, J.M. MacLaren and S. Lao, In High-Temperature Ordered Intermetallic alloys IV, ed. L.A. Johnson, D.E. Pope and J.O. Stiegler, Mater. Res. Soc., Pittsburgh, 1991, p. 715.
[27] G. Hug, A. Loiseau and P. Veyssiere, Phil. Mag. A, 1988, 57, 499.
[28] P.M. Hazzledine, B.K. Kad, H.L. Fraser and D.M. Dimiduk, presented at the 1992 MRS Spring Meeting, San Francisco, CA, 1993, in press.
[29] T. Hanamura, R. Uemori, M. Tanino and H. Morikawa, Ultramicroscopy, 1991, 39, 86.